PHILOSOPHICAL TRANSACTIONS A

rsta.royalsocietypublishing.org

Review

Cite this article: Goldstein ML, Wicks RT, Perri S, Sahraoui F. 2015 Kinetic scale turbulence and dissipation in the solar wind: key observational results and future outlook. *Phil. Trans. R. Soc. A* **373**: 20140147.
http://dx.doi.org/10.1098/rsta.2014.0147

Accepted: 13 February 2015

One contribution of 11 to a theme issue 'Dissipation and heating in solar wind turbulence'.

Subject Areas:
plasma physics, astrophysics, complexity

Keywords:
solar wind, turbulence, plasma heating, turbulent dissipation

Author for correspondence:
M. L. Goldstein
e-mail: melvyn.l.goldstein@nasa.gov

Kinetic scale turbulence and dissipation in the solar wind: key observational results and future outlook

M. L. Goldstein[1], R. T. Wicks[1,2], S. Perri[3] and F. Sahraoui[4]

[1]Code 672, NASA Goddard Space Flight Center, Greenbelt, MD 20771, USA
[2]GPHI, Astronomy Department, University of Maryland, College Park, MD 20742, USA
[3]Dipartimento di Fisica, Università della Calabria, Rende 87036, Italy
[4]Laboratoire de Physique des Plasmas, CNRS-UPMC, Ecole Polytechnique, Route de Saclay, Palaiseau 91128, France

Turbulence is ubiquitous in the solar wind. Turbulence causes kinetic and magnetic energy to cascade to small scales where they are eventually dissipated, adding heat to the plasma. The details of how this occurs are not well understood. This article reviews the evidence for turbulent dissipation and examines various diagnostics for identifying solar wind regions where dissipation is occurring. We also discuss how future missions will further enhance our understanding of the importance of turbulence to solar wind dynamics.

1. Background

The solar wind is the outer atmosphere of the Sun, which is flowing outwards from the solar corona at supersonic and super-Alfvénic speeds, i.e. the solar wind speed, V_{SW}, exceeds both the speed of sound and the speed of the characteristic plasma mode, the Alfvén speed, given by $V_A = B/\sqrt{(4\pi\rho)}$, where B is the magnitude of the local magnetic field and ρ is the mass density. The equation is written in cgs units and ρ includes all of the ions that comprise the solar wind. Typically, 80% of the mass is carried by protons and virtually all of the rest is due to He

THE ROYAL SOCIETY PUBLISHING

in the form of alpha particles. The alpha to proton mass density ratio is highly variable and so for any particular interval is likely to differ from the canonical value of 20% [1].

The existence of the solar wind was predicted in 1958 by Parker [2] and discovered at the dawn of the space age by Gringauz [3] in data obtained by the *Luna* spacecraft and by Neugebauer & Snyder [4] using data from *Mariner* 2. Early observations soon indicated that the solar wind contains magnetohydrodynamic (MHD) waves (in particular, Alfvén waves) [5,6] but in many other respects the fluctuations resemble fluid turbulence [7,8]. Coleman's [8] paper inspired a lively debate as to whether or not the solar wind is best described as a medium consisting of non-interacting 'waves' or as a turbulent magnetofluid. One of the important observational aspects of the debate was the observation that the fluctuations in the magnetic and velocity fields are often nearly completely aligned so that $\delta\mathbf{v} = \mp\delta\mathbf{b}/\sqrt{(4\pi\rho)}$, where $\delta\mathbf{b}$ and $\delta\mathbf{v}$ are the (vector) fluctuations of the magnetic and velocity fields, respectively. If one assumes that the fluctuations are totally aligned so that the equality is satisfied, then the ideal (i.e. zero dissipation) incompressible equations of MHD have no nonlinear terms and the equality is an exact solution (also see the discussion in [9]).[1] In such a scenario, there cannot be any actively evolving turbulence. On the other hand, as pointed out by Coleman, the power spectra of the magnetic fluctuations resemble those seen in Navier–Stokes (incompressible) turbulence and the shape of those spectra is well described by Kolmogorov's 1941 theory [10]. The cross helicity, defined as $H_c = \frac{1}{2}\int \mathrm{d}^3x\ \mathbf{v}\cdot\mathbf{b}$, quantifies this correlation.

(a) Early evidence for dissipation and turbulent heating

Further evidence that the solar wind is a turbulent magnetofluid was presented by Matthaeus & Goldstein [11], who pointed out that for (stationary) intervals spanning several days, the spectrum of magnetic fluctuations could be very close to the Kolmogorov $-\frac{5}{3}$ power-law slope characteristic of turbulent fluids (e.g. Grant *et al.* [12]). A more intensive exploration of the 'waves' versus 'turbulence' question was carried out by Roberts & Goldstein [13,14], who concluded that both points of view had varying amounts of validity. In their analyses of intervals that spanned the heliosphere from 0.3 to 10 astronomical units (AU) using data from the two *Helios* spacecraft together with data from *Voyager* 1 and 2, they observed that for highly Alfvénic fluctuations [6] characterized by a high alignment between velocity and magnetic fluctuations (in the sense that the cross helicity was nearly maximal) there was little evidence of turbulent evolution, especially in fast solar wind out to 1 AU. (High cross helicity, along with strong correlations of other variables, tends to reduce the nonlinear terms in the MHD equations—see the discussion in [9].) However, in general, the degree of alignment tended to decrease with heliocentric distance. The evolution was more rapid for the short-scale fluctuations and slower for the larger-scale ones. Furthermore, the decline in cross helicity tended to be more rapid and larger for intervals that had been 'stirred' by co-rotating interaction regions, shock waves or other energetic phenomena. These results suggested that Alfvénic fluctuations were generated near the Sun followed by dynamical evolution caused by nonlinear couplings induced by the presence of large-scale structures as the wind flowed outwards into the heliosphere.

In a turbulent medium, energy injected at large scales must eventually dissipate at small scales. In a magnetofluid, the dissipation can occur in a number of ways. In *collisional* magnetofluids, dissipation occurs via viscous effects originating at the molecular level due to collisions between particles as well as by Joule heating (*electrical resistivity*). In *collisionless* plasmas, such as those encountered in near-Earth space, wave–particle interactions play a key role in mediating energy transfers between fields and particles. In the context of wave–particle interactions, one can imagine a scenario where the cascade of fluctuations to smaller and smaller scales reaches the point where the thermal plasma can be in resonance with the fluctuations and the resultant wave–particle processes can damp the electromagnetic energy, heating the plasma [15,16]. A related, but more 'nonlinear', picture might involve discontinuities, especially rotational, and/or current

[1] Anti-correlation implies 'waves' propagating parallel to the background magnetic field while positive correlation implies propagation anti-parallel to the field.

sheets, where magnetic reconnection can occur. The interaction of the (demagnetized) particles with the small-scale fields would also result in plasma heating. As we shall point out below, differentiating between those two scenarios with the present instrumentation on spacecraft is not an easy task.

The dissipation of the turbulence due to velocity shears, wave damping, etc., will heat the plasma (see Coleman [8] for an early quantitative estimate of this process that was further developed by Hollweg [17]). Tu & Chen [18] used *Helios* data to investigate the radial evolution and concluded that turbulent dissipation fitted the observations quite well, unlike viscous dissipation, which failed to account for the observations by eight orders of magnitude.

The spherical expansion of the solar wind implies that it will cool adiabatically. That cooling competes with heating due to turbulent dissipation. Adiabatic cooling leads to a temperature decrease with radius R that goes as $R^{-4/3}$. Gazis *et al.* [19,20] compared observations made by *Voyager* 1 as it travelled from 1 AU to nearly 10 AU with data from a very similar instrument on *IMP* 8 in Earth orbit. They showed that the decrease in plasma temperature was much slower than that predicted by the adiabatic law, decreasing only as $R^{-2/3}$. Gazis *et al.* surmised that the heating might be a consequence of thermal processes such as the addition of a heat flux due to heat conduction.

Verma *et al.* [21] investigated the possibility that the observed heating was due to the dissipation of the *in situ* turbulence. They showed that turbulent dissipation could provide sufficient heat to account for the observed slower-than-adiabatic radial dependence of the temperature. Verma *et al.* further concluded that the estimated heating was more consistent with the expectations of a Kolmogorov-like turbulent fluid cascade rather than a Kraichnan–Iroshnikov-like magnetofluid cascade [22,23]. However, the heating in the model was not quite adequate to account fully for the observed temperature dependence and the authors concluded that other processes, such as heat flux, might be involved.[2] To add to the complexity of this problem, Tu [24] found no evidence for turbulent heating in the time period he studied.

In the latest effort to include turbulent heating in the context of a global model of the solar wind [25], electrons, protons and interstellar pick-up protons were all given separate energy equations and the electron heat flux was incorporated using the approximation first derived by Hollweg [26,27]. While that model shows that turbulence does heat the solar wind, the paucity of observations in the outer heliosphere, coupled with the fact that the *Voyager* plasma instrument cannot see the pick-up proton temperature component, makes it difficult to draw definitive conclusions. Furthermore, the trajectory of *Voyager* 1 takes it out of the ecliptic plane and the model shows that high-latitude regions are hotter than is the ecliptic, which tends to obscure the effects of heating by turbulence. Consequently, it is important to examine in detail *in situ* measurements of the dissipation range of the turbulence to ascertain the detailed physical processes that heat the wind.

2. Heating and dissipation of solar wind turbulence

(a) Heating

One way to estimate heating of the solar wind is to measure the rate of the turbulent energy cascade [28,29], which is provided by measurements of the third moment of the fluctuations. The 10 years of solar wind data from 1998 to 2007 from the *Advanced Composition Explorer* (*ACE*) at 1 AU provided MacBride *et al.* [28] the opportunity to use third-order-moment theory by providing good convergence and statistically significant datasets [30]. MacBride *et al.* concluded that the total turbulent energy injection and dissipation rates derived agree with the *in situ* heating of the solar wind that is inferred from the temperature gradient. (For a discussion of the accuracy of third-order moments, see Podesta *et al.* [31].) The consistently high values of the MHD cascade

[2]One should keep in mind, however, that, in the solar wind, the heat flux is primarily carried by electrons and their coupling to the proton fluid is very weak, so the physical mechanism by which heat flux might contribute to the bulk ion temperature of the solar wind is unclear.

rates found by Stawarz *et al.* [29] indicated that the turbulent cascade deposited more energy than required for the observed proton heating, suggesting that the excess energy could potentially go towards heating electrons—which would be consistent with the Landau damping scenario mentioned above [32] (also see Sahraoui *et al.* [33]). In related work, Coburn *et al.* [30] found that the solar wind during the last solar minimum was still very turbulent, although the cascade rate of the turbulence was lower, perhaps owing to the paucity of high-latitude (coronal hole) sources.

In situations where the cross helicity of the fluctuations is large, one expects that the cascade rate should be slower than when the cross helicity is small because maximal cross helicity reduces all nonlinear interactions in the (incompressible, ideal) MHD equations (as mentioned above and as discussed in Matthaeus *et al.* [9]. Stawarz *et al.* [34] examined that expectation (also see [35]). They found that time periods containing large-helicity states indicated a significant *back-transfer* of energy from small to large scales. This back-transfer reinforced the dominance of the outward-propagating fluctuations. They suggested that the back-transfer might provide a partial explanation for large-helicity states in the solar wind, but acknowledged that such a back-transfer could not continue for long before it would come into conflict with the observed temperature of the solar wind at 1 AU. The mechanism for such a process is unclear, as in three-dimensional MHD turbulence energy cascades forwards and there is no observational evidence for any dynamical alignment of the velocity and magnetic fluctuations [13,14,36]. Furthermore, their conclusion has been criticized by Podesta [37], who suggested that Stawarz *et al.* may have underestimated the statistical errors inherent in their use of third-order moments.

Osman *et al.* [38] compared solar wind *ACE* data with results from MHD simulations and showed that regions characterized by high magnetic energy fluctuations (as detected by the partial variance of increments, or PVI) associated with the presence of coherent structures exhibit a higher mean ion temperature as compared with the ambient solar wind, suggesting that such structures can be potential sources of local plasma heating. (The reader is referred to [9, §5] for a detailed introduction to the PVI method.) By contrast, Borovsky & Denton [39], selecting hundreds of current sheets in the *ACE* magnetic field data, found no evidence of an enhancement in proton and electron temperatures during current sheet crossings. Further investigations are needed to resolve that apparent conflict.

The analyses that rely on the third-order law implicitly require that the turbulence be incompressible. However, the solar wind is not truly incompressible and, thus, errors in the observations of third-order moments, owing to their slow convergence to a mean, severely limit their use in the solar wind [31]. Coburn *et al.* [30] and Stawarz *et al.* [29,34] assumed that the computed third-order moments were accurate everywhere, and that the slow convergence was due to the highly variable nature of the third moment rather than to any large uncertainty in the observations. With this proviso, their work stands; however, this assumption has not been proven, and so there remains an unknown uncertainty on these results, making them inconclusive at the current time.

(b) Dissipation

Following the early and general investigations of the possible role of turbulence and other processes in heating the solar wind, interest turned to describing the dissipation range itself. The largest scales where dissipation is suspected to be happening are comparable to the gyroradius of a thermal proton, $\rho_p = V_{th,p}/\Omega_p$ (where $V_{th,p}$ is the proton thermal speed and Ω_p is the proton gyrofrequency), or to the proton inertial length, $\lambda_p = c/\omega_{pp}$ (where ω_{pp} is the proton plasma frequency). These scales are typically between 100 and 1000 km in the solar wind at 1 AU and so are convected past a spacecraft in a couple of seconds or less at typical solar wind speeds. Thus, observations able to resolve the dissipation range must be made at cadences of the order of or faster than 1 Hz, which requires high-time-resolution magnetometer and plasma data.

In one of the pioneering studies of the dissipation range magnetic field, Leamon *et al.* [40] noted that the approach to the dissipation range at 1 AU sets in at spacecraft-frame frequencies of a few tenths of a hertz, a range accessible to magnetometers on *Wind*, *Voyager* and many other

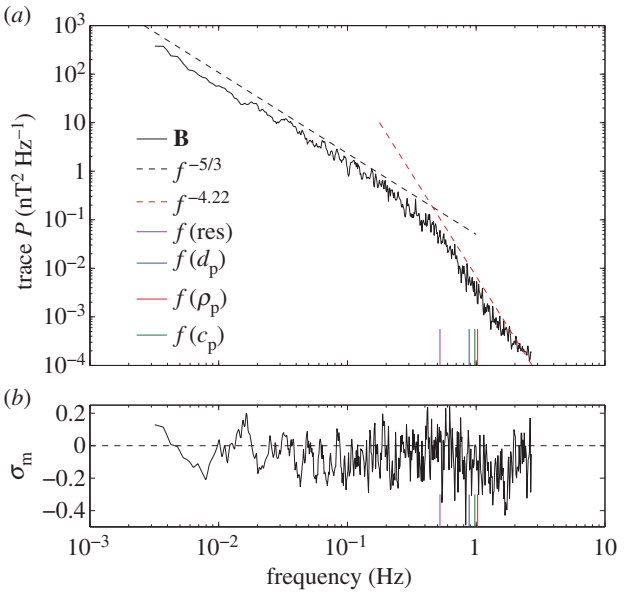

Figure 1. An interplanetary power spectrum from the Wind spacecraft on 30 January 1995, 1300–1400 UT, showing the inertial range and the beginning of the dissipation range. (*a*) Trace of the spectral matrix with a break at ∼0.4 Hz where the dissipation range sets in. (*b*) The corresponding magnetic helicity spectrum [41] (cf. [40, fig. 1]). The (Doppler-shifted) physical frequencies are indicated as coloured vertical lines on the frequency scale. Here $f(\mathrm{res}) = V_{SW}\Omega_{ci}/(V_A + V_{th})$ (purple) is the parallel (to **B**) cyclotron wave resonance as described in Bruno & Trenchi [42], where Ω_{ci} is the proton cyclotron frequency, V_A is the Alfvén speed and V_{th} is the thermal speed parallel to **B**; $f(d_p) = V_{SW}\Omega_{pi}/c$ (blue) is the proton inertial length, where Ω_{pi} is the proton plasma frequency; $f_{\rho_p} = V_{SW}\Omega_{ci}/V_{th}$ (red) is the proton gyroradius; and $f(c_p) = \Omega_{ci}(1 + V_{SW}/V_A)$ (green) is the Doppler-shifted proton cyclotron frequency.

spacecraft (cf. figure 1). The dissipation range should be characterized by a steepening of the power spectrum and, often, a change in the polarization or magnetic helicity spectrum of the magnetic fluctuations [43].[3] Whether or not the break seen at these proton scales actually reflects dissipation is difficult to determine despite the fact that, at these scales and smaller, kinetic effects are expected to couple the fluctuations to the background plasma, removing magnetic energy and thus heating the background plasma. Cyclotron damping and/or Landau damping may well be important, but dispersion due to finite Larmor radius effects, as reflected in either Hall MHD or gyrokinetic treatments [45], also leads to spectral breaks at these same ion scales. (For related ideas on the relationship between plasma distribution functions and dissipation, the reader is referred to [46–48].) It is clear, however, that to determine the physics of what is actually happening will require more and higher-time-resolution data in addition to detailed analyses.

Analysis of *Wind* data by Leamon *et al.* [40] showed that interplanetary turbulence consisting solely of parallel-propagating waves, such as Alfvén waves, was inconsistent with the observations. Two possibilities emerged: the fraction of the MHD turbulence that was two-dimensional could be interacting with ambient plasma (although the scales being analysed may have been too small for the application of MHD theory). Alternatively, kinetic Alfvén waves (KAWs) propagating at large angles to the background magnetic field were also consistent with the observations. KAWs are often observed to be quasi-oblique and nearly stationary (and, hence, quasi-two-dimensional).[4]

[3]The magnetic helicity represents the handedness of the fluctuations; see e.g. Moffatt [44] and Matthaeus & Goldstein [11].

[4]We will return to these ideas below when we discuss higher-time-resolution studies using search coil magnetometer data from the STAFF experiment on *Cluster*—data that showed breaks and/or curvature in the spectrum at scales much smaller than those associated with ion-scale physics.

In a subsequent paper [15], the authors examined the relative importance of cyclotron damping of quasi-parallel Alfvénic fluctuations and kinetic non-resonant dissipation. They concluded that, for the intervals analysed, the two processes were roughly equal, thus accounting for the observations that cyclotron damping, as indicated by magnetic helicity analyses, was never complete (cf. [40,43]). Furthermore, a study of the general characteristics of damping of KAWs [32] indicated that Landau damping by solar wind thermal protons and electrons must be important in determining the extent to which turbulent dissipation could heat the solar wind (for a recent analysis of the possible role of both whistler waves and kinetic Alfvén waves in the dissipation regime, see [49]).

Several studies of ion cyclotron waves in the solar wind have recently been published using data from the *STEREO* spacecraft. In the first, He *et al.* [50] explored the possible existence of Alfvén cyclotron waves and their coexistence with obliquely propagating KAWs or whistler waves. In a related study, He *et al.* [51] looked into the question of whether the beginning of the dissipation range of the spectrum was dominated by Alfvén, cyclotron or fast mode whistler waves. They concluded that the observed polarization of the magnetic fluctuations indicated that oblique KAWs dominated the spectrum near the spectral break. The interaction between magnetic helicity and instabilities is unclear, as there are many observed intervals of solar wind flow in which the temperature anisotropy and plasma β are $\sim$1 and so are completely stable to the excitation of cyclotron waves. In another study, Jian *et al.* [52] have reported extensive occurrences of ion cyclotron waves in the solar wind—the implications of these observations to solar wind heating and other processes are at present unclear. For a discussion of the possible role of alpha particles on instabilities that affect the population of solar wind fluctuations, the reader is referred to Podesta & Gary [53]. Further evidence that near the dissipation range the fluctuations are primarily oblique to the local magnetic field was published recently by Klein *et al.* [54] using data from *Ulysses*. Klein *et al.* concluded that some 95% of the fluctuating power near the dissipation scales was contained in perpendicular Alfvénic fluctuations, i.e. kinetic Alfvén waves.

The question of the role of cyclotron damping was also addressed from a different point of view by Leamon *et al.* [55] (also see [56,57]), where, instead of kinetic processes including Landau damping of KAWs, the comparison was with dissipation arising from the (perpendicular) turbulent cascade at the ion inertial scale evolving into thin current sheets that were the sites of magnetic reconnection (also see Osman *et al.* [58], who investigated the connection between the energy cascade rate of the turbulence and kinetic effects driven by temperature anisotropies). In the corona, at least (and maybe the solar wind, too), the conclusion was that a significant fraction of dissipation resulted from a perpendicular cascade and small-scale reconnection. In the solar wind, to study this regime requires use of high-frequency search coil data, as discussed in the following sections.[5]

(c) Determination of the scale of the spectral break between magnetohydrodynamic and kinetic turbulence

Since the physical mechanism that dissipates magnetic energy in the solar wind is still unclear, recent studies have tried to shed light on this question by exploring more deeply the physical processes operating where the Kolmogorov-like spectrum breaks and a steeper spectrum appears [40,75] (cf. figure 1). In this range, kinetic effects must be taken into account, and relating the break position to a physical scale is helpful for clarifying the process responsible for the high-frequency turbulent cascade observed.

Different mechanisms have been invoked to explain the kinetic range of the turbulent cascade. One possibility is that the 'high-frequency' (in the spacecraft frame of reference) range reflects a cascade of KAWs propagating almost perpendicularly to the mean magnetic field [75–77]

[5]In this review, we are concentrating on the description of the kinetic scale processes that dissipate the turbulence and heat the ambient fluid. The closely related subject of how waves and turbulence might accelerate and heat the corona cannot be addressed here and the reader is referred to the review in this issue by Cranmer *et al.* [59] and to other work that concentrates on that topic (e.g. [16,57,60–74]).

beginning at the proton gyroradius. Another scenario envisages the proton cyclotron damping of Alfvénic fluctuations at scales of the ion inertial length, so that the high-frequency range has been interpreted as a cascade of whistler waves [78]. Furthermore, Hall MHD turbulence [79,80] and the generation of current sheets perpendicular to the mean field [81] also involve a spectral break near the proton inertial length.

Recently, Markovskii *et al.* [82], analysing a large sample of *ACE* solar wind data, have shown that the high-frequency spectral break is well correlated not with a single typical plasma scale but probably with a combination of scales and with the amplitudes of the magnetic fluctuations at those scales. This evidence suggests that the high-frequency cascade could be controlled by several processes. Using 1 s resolution *Ulysses* data obtained at radial distances greater than 1 AU together with 0.5 s resolution *MESSENGER* data for radial distances less than 1 AU, Perri *et al.* [83] studied the radial evolution of the high-frequency spectral break f_b and concluded that the break frequency did not show any significant radial variation, perhaps indicating that the spectral break reflected a coronal imprint.

On the other hand, Bruno & Trenchi [42], using a combination of *MESSENGER*, *Wind* and *Ulysses* data during radial alignments of the satellites, concluded that there was a clear radial dependence, i.e. $f_b \sim R^{-1.09}$, and showed good agreement between the scaling of the observed break wavenumber and the scaling of the wavenumber corresponding to the resonance condition for parallel-propagating Alfvén waves [40], a result consistent neither with the damping of kinetic Alfvén waves [76] nor with Hall MHD effects [84,85].

In another look into the spectral break problem, Bourouaine *et al.* [86] used magnetometer data from *Helios* 2 and *Ulysses* to look at the radial variation of the magnetic power spectrum from 0.3 to 0.9 AU. The analysis focused on fast solar wind and the magnetic field spectral data extended up to 2 Hz. The *Ulysses* data indicated that, taking into account the two-dimensional nature of the turbulent fluctuations, the spatial scale corresponding to the frequency of the spectral break followed the proton inertial scale with distance. The observations indicated that the spectral break at the proton inertial scale might be related to the Hall effect or was controlled by ion cyclotron damping of obliquely propagating fluctuations or by the formation of current sheets (which could be responsible for ion heating through magnetic reconnection).

In a recent paper, Chen *et al.* [87] investigated the scale at which the first spectral break occurred in the plasma frame by dividing the intervals studied into groups in which the perpendicular ion plasma beta satisfied either $\beta_\perp \gg 1$ or $\beta_\perp \ll 1$. The conclusion was that for $\beta_\perp \ll 1$ the break occurred at d_i while for $\beta_\perp \gg 1$ the break was at ρ_i. A recently published theoretical analysis [88] has pointed out the important role played by the magnetic helicity [41,44] in influencing the spectral index of magnetic power at both d_i and ρ_i scales.

Together, these analyses emphasize the need for new measurements, such as from *Solar Orbiter* and *Solar Probe Plus*, as well as from new missions to resolve this issue. Thus, at this time there is no definitive conclusion that can be drawn.

3. Determination of the three-dimensional properties of solar wind turbulence

A key measurement to make in turbulent magnetized plasmas is the determination of the gradients along and perpendicular to the mean magnetic field $\langle \mathbf{B}(t) \rangle = \mathbf{B}_0$. In Fourier space, this is equivalent to measuring the wavenumber spectra of the turbulence parallel and perpendicular to $\mathbf{B}_0$, i.e. $P(k_\parallel)$ and $P(k_\perp)$. This information is crucial for the direct identification of the plasma modes that carry the turbulence cascade. Such spectra also allow one to identify the nature of the wave–particle interactions that might be operating and that may be responsible for the local plasma heating.[6] Unfortunately, measuring the full three-dimensional **k**-vector space of turbulence in the solar wind is challenging, especially since single-spacecraft data allow one to

[6]One should keep in mind as discussed below that the Fourier transform of a series of discontinuities may also produce similar looking power spectra.

measure only the component of the **k**-vector along the flow direction under the Taylor frozen-in flow assumption [89].

When data from only a single spacecraft are available, many approaches have been developed to measure the three-dimensional distribution of power in k-space. The techniques use either structure functions or wavelets to estimate the time- and scale-dependent amplitudes of fluctuations along with the direction of the 'local' magnetic field. The techniques require large deflections of the magnetic field to ensure sampling many angles relative to the local field direction. However, the techniques must also assume stationarity of the data. Most studies have focused on the inertial range of turbulence and have shown that the spectral scaling of fluctuations is anisotropic with respect to the local field direction, meaning that anisotropy of power grows as the turbulence cascades to smaller scales. As the cascade progresses, power in fluctuations perpendicular to the local magnetic field tends to dominate over power in the parallel direction [90–94]. At least in a statistical sense, anisotropies generated in the inertial range will impact the dissipation and heating of the solar wind by determining the form of energy-containing fluctuations that reach scales where dissipation occurs. There is additional evidence that this anisotropy persists and even grows in the ion kinetic regime [95].

A three-dimensional measurement requires a minimum of four probes placed at the vertices of a fairly regular tetrahedron. The probes must simultaneously measure the fluctuating magnetic field. The ESA–NASA *Cluster* mission [96] is the first space mission designed to measure three-dimensional structures in space, including the **k**-vectors of turbulence. These three-dimensional measurements have provided insight into the anisotropy of the turbulence and the actual mechanisms of energy dissipation. Analysis of the magnetic field data has employed the k-filtering (or wave telescope) technique [97–101], which is an interferometric method designed for multipoint measurements. It combines several time series recorded simultaneously at different points in space to estimate the four-dimensional function $P(\omega, \mathbf{k})$ under the assumption that the time series is both stationary [102] and spatially homogeneous.

An example of applying the k-filtering technique to *Cluster* data can be found in Sahraoui *et al.* [33]. The study indicated that the turbulence was strongly anisotropic at kinetic scales with $k_\parallel/k_\perp \ll 1$, and was dominated by KAWs with frequencies $\omega/\omega_{ci} \ll 1$, where $\omega_{ci} = eB/m_p c$ is the proton gyrofrequency. Linear solutions of the Maxwell–Vlasov equations indicated that under those conditions energy dissipation was likely to happen through the Landau damping rather than via cyclotron resonance (see figure 2), primarily because the fluctuation wavevectors were too oblique to the magnetic field to resonate with solar wind protons. The very low frequency in the plasma frame of reference also implied that the 'fluctuations' were essentially stationary. This aspect of the turbulence was investigated further [103] using the same dataset. That analysis showed the presence of current sheets with scales of the order of or smaller than the ion Larmor radius, suggesting that magnetic reconnection might be important within those current sheets in dissipating the energy. Similar fluctuations and current sheets have been found in *Cluster* data in both Earth's magnetosheath [104,105] and magnetotail regions [106,107]. The coexistence of wave-like signatures and current sheets is an exciting topic of theoretical research that warrants further investigation.

The multi-spacecraft *Cluster* formation has also been used to investigate the three-dimensional structure of solar wind magnetic field fluctuations at small inertial range scales and in the proton kinetic regime. Narita *et al.* [108] used k-filtering to find the three-dimensional shape of the power distribution at small scales in the inertial range. Chen *et al.* [109] made a similar measurement using structure functions with data from a single spacecraft. Both results show highly anisotropic structures with a flattened pancake shape, elongated along the magnetic field direction with most power, or thinnest dimension, in the perpendicular direction aligned with the maximum variance direction in the mean-field-perpendicular plane. Chen *et al.* [110] also looked at the spatial anisotropy at ion kinetic scales using all four *Cluster* spacecraft. They concluded that the power and scaling of the anisotropy were similar to that predicted for KAWs.

An analysis of five years of *Cluster* (high time resolution) STAFF data [111] found evidence that about 10% of the fluctuations show narrow-band, right-handed, circularly polarized fluctuations,

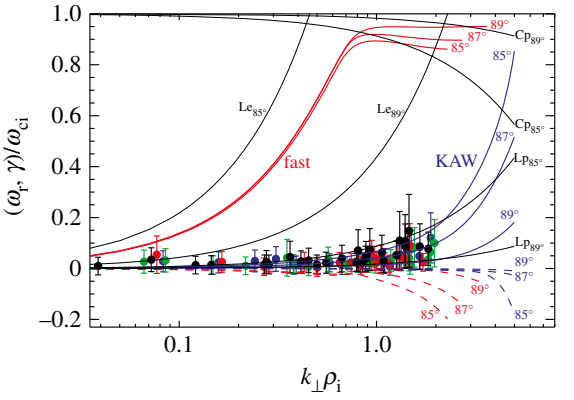

Figure 2. Observed dispersion relations (dots) at kinetic scales in the solar wind, with estimated error bars, compared with linear solutions of the Maxwell–Vlasov equations for three observed angles Θ_{kB} (the dashed lines are the damping rates). The black curves are the different kinetic resonances (Landau and cyclotron effects). (Reproduced with permission from [33].)

with wavevectors quasi-parallel to the mean magnetic field, superimposed on the spectrum of the permanent background turbulence. These observations provide evidence that when the electron parallel beta factor $\beta_{e\parallel} \geq 3$, the whistler waves are present at the heat flux threshold of the whistler heat flux instability. The presence of these whistlers indicates that the whistler heat flux instability may be contributing to the regulation of the solar wind heat flux, at least for $\beta_{e\parallel} \geq 3$, in slow wind, at 1 AU.

4. Observations of electron scale turbulence

Observations of AC magnetic fields from the search coil magnetometers on *Cluster* have been combined with the DC flux gate magnetometer measurements to provide broadband spectra from mHz to kHz in the spacecraft frame of reference (figure 3 [75,110,112,113]). The observations show a steepening of the power spectrum of the magnetic field between proton and electron scales (to approx. −2.5) with a further steepening of the spectrum (to approx. −3.8) at the highest frequencies sampled.

The high-time-resolution electric and magnetic field measurements on *Cluster* are available up to ∼180 Hz and enable, for the first time, exploration of electron scale turbulence [75,114–116]. These observations show that magnetic energy has a spectrum that extends towards scales of order ρ_e, where dissipation becomes even more important as evidenced by the further dramatic steepening of the spectra (ρ_e is the electron gyroradius, defined as V_{th_e}/ω_{ce} where V_{th_e} is the thermal speed of the electron distribution and ω_{ce} is the electron gyrofrequency).

In addition to *Cluster*, the *Spektr-R* spacecraft is able to measure ion distribution functions with a cadence of 31 ms [117,118]. The Fourier transform of the velocity, density and temperature time series are qualitatively similar to spectra produced from the magnetic field. All variables have a $\sim f^{-5/3}$ scaling in the inertial range, with a spectral break at a few tenths of a hertz to a more variable but steeper scaling between $f^{-2.5}$ and $f^{-3.5}$. In many cases [117,118], we observe a noticeable peak in the density and velocity spectra at the break scale, similar to a peak observed simultaneously in upstream (*Wind* MFI) magnetic field spectra.

Another approach to obtaining high-frequency ion density spectra in the solar wind is to measure the spacecraft potential. This has most recently been done using *THEMIS* [119], for which the electric potential can be measured at a cadence of 8192 samples per second. However, the conversion of the potential data into electron density is made complicated by the highly variable charging of the spacecraft by the solar wind. The resulting spectra are similar to the magnetic field spectra described above and are consistent with being dominated by KAW turbulence.

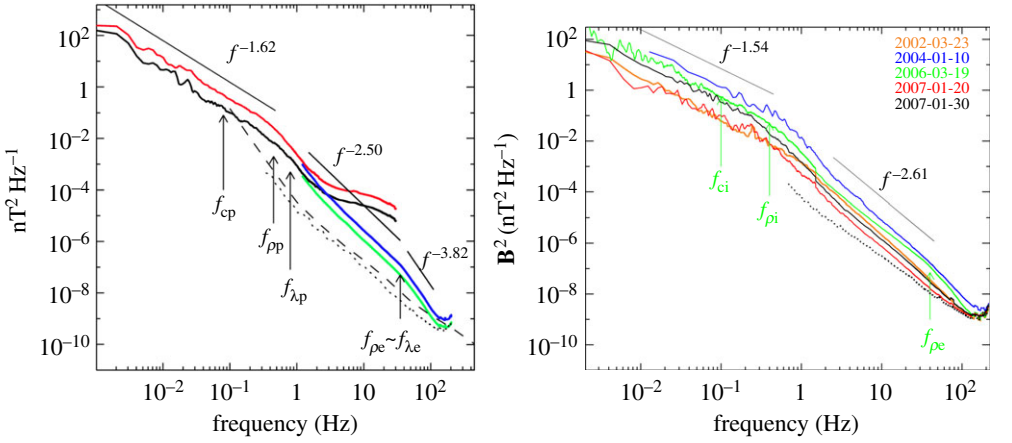

Figure 3. (*a*) High cadence magnetic field spectra observed by combining data from the *Cluster* FGM and STAFF instruments. The different ranges of each instrument are highlighted showing how such a wide range of frequencies is covered. Proton and electron scales are marked and correspond to locations where the spectra steepen. Reproduced from [75, fig. 2]. (*b*) Power spectra of **B** measured by FGM and STAFF over five different intervals. The straight black lines are direct power-law fits of the spectra. Vertical arrows are the Doppler-shifted proton gyrofrequency and proton and electron gyroradii.

Additional studies of solar wind and magnetospheric turbulence have used alternative methods. Anisotropy has been investigated using wavelet techniques on data from single spacecraft [113] and structure functions from non-tetrahedral *Cluster* formations [110]. Those studies used the 'local mean field', that is, the mean magnetic field is measured over the envelope of the wavelet or structure function that is used to measure the fluctuations. This provides a scale-dependent mean magnetic field that allows many different angles to the mean field to be measured so long as a sufficiently long interval of stationary solar wind is processed. The results of these studies show that power anisotropy decreases (i.e. the fluctuations become less transverse, relative to the local mean field) [75,114], whereas the spectral index anisotropy increases in the dissipation range [110]. These analyses also support the idea that dissipation range fluctuations are dominated by KAWs.

Recent observations have motivated intensive research into electron scale turbulence both theoretically and numerically [120–127]. However, the underlying physics remains controversial primarily owing to the fact that the available observations are few and theoretical and numerical work has been extended to those small scales only recently. One issue concerns the scaling of the magnetic energy spectra down to and below ρ_e. Sahraoui *et al.* [75] first reported a power-law cascade $f_{sc}^{-2.8}$ down to f_{ρ_e}, where a clear spectral break is observed, followed by another power law close to f_{sc}^{-4} (f_{ρ_e} is the frequency in the spacecraft frame corresponding to the electron gyroscale when the Taylor frozen-in flow assumption is used). This has been confirmed in a survey of 10 years of STAFF waveform data in the free-streaming solar wind [128]. On the other hand, Alexandrova *et al.* [112,115], using STAFF-Spectrum Analyser (STAFF-SA) data, have reported exponential scaling in the scale range $k\rho_e \sim [0.03, 3]$.

Another controversy concerns the nature of the plasma modes that carry the turbulence cascade down to electron scales. Two main channels have been discussed: KAW [33,75,129,130] and the whistler turbulence [125]. There is growing evidence, as discussed above, that the dominant component of the turbulence is consistent with KAWs. This has been shown using the estimation of the 'phase speed' E/B [75,129,131], the dispersion relation obtained from the k-filtering [33], the magnetic compressibility [113] and the density fluctuations [130]. Podesta [132] also concluded from several independent analyses that kinetic Alfvénic fluctuations are generally present in the solar wind. However, apart from the work using *k-filtering* [33], most other studies assume that the Taylor frozen-in flow hypothesis is satisfied. While this hypothesis is often valid

at MHD scales in the solar wind, it can fail for dispersive waves that have high phase speeds, such as parallel-propagating whistlers [133], and for intervals for which the fluctuation wavevectors are nearly orthogonal to the direction of solar wind flow.

The third point of controversy concerns the relative importance of the two paradigms used to describe turbulence at small scales: viz., the wave-like picture (KAWs, whistler waves, etc.) versus coherent structures (e.g. current sheets), and the possibility of the coexistence of both waves and structures in the turbulent mix. This question is closely related to the true nature of the turbulence cascade and to the appropriate theoretical approach for describing turbulence at kinetic scales—areas that will be addressed experimentally with the forthcoming launch of the *Magnetospheric Multiscale* (*MMS*) mission and are being intensively studied using numerical simulations and theoretical analyses.

5. Magnetic field discontinuities and intermittency

The solar wind is characterized by abrupt changes in the magnetic field, i.e. *discontinuities*, over a very broad range of time scales [103,134–136]. The properties of those time variations can be very different, so that according to their characteristics they have been interpreted as boundaries between flux tubes originating in the photosphere [137–139] or as current sheets that form as a consequence of the turbulent cascade [140] (also see [9]). The use of 450 vectors per second resolution STAFF data on *Cluster* allowed Perri *et al.* [103] to study the spatial properties of the magnetic field fluctuations, including current sheets, at scales close to and smaller than the proton inertial length. Those structures were seen as abrupt changes in the magnetic field direction and/or sharp decreases in the magnetic field magnitude (left panels of figure 4). The current sheet occurred at a time when the four *Cluster* spacecraft formed a regular tetrahedron with an average separation of 200 km.

Figure 4 displays an almost simultaneous observation of a current sheet by both *Cluster* 2 (red dashed line) and *Cluster* 4 (blue solid line) when the spacecraft separation was only 20 km along the flow direction. The angle of rotation $\alpha(t,\tau) = \arccos(\mathbf{B}(t)\cdot\mathbf{B}(t+\tau))/(|\mathbf{B}(t)||\mathbf{B}(t+\tau)|)$, computed at a time scale $\tau = 0.035$ s, increases in both *Cluster* 2 and *Cluster* 4. The magnetic field components are plotted in the local minimum variance reference frame (*LMN*) to better address signatures of the current sheet crossing (see figure legend). The L and N components lie in the current sheet plane along the maximum and the minimum variance directions, respectively. The magnetic field along L smoothly changes sign, while the component along N is almost zero. The intermediate variance M component is out of the plane and tends to show a bipolar signature, which is typical of the Hall field. The discontinuity has a spatial scale of $d \sim 38$ km (very localized), which means for that interval $\lambda_p \sim 1.6d$ and $\rho_p \sim 1.9d$. A comparison with proton scale current sheets forming during a two-dimensional Hall MHD simulation of freely decaying turbulence gives qualitative agreement with solar wind observations (see right panels in figure 4), although discontinuities close to electron scales cannot be resolved. Notice that current sheets in the Hall MHD simulation are sites of magnetic reconnection. A challenging outlook is to find whether thin current sheets observed in the solar wind between proton and electron scales can be sites of magnetic energy dissipation via reconnection. This would be possible with high-resolution electric field data with a high signal-to-noise ratio. The present EFW data on *Cluster* allow for scientific analysis up to about 4–5 Hz, which is insufficient to resolve electron scale structures.

The presence of small-scale magnetic discontinuities seems to be a peculiar aspect of the magnetic field in the solar wind and has been detected both in the inner heliosphere and at 1 AU [141] by several methods, as the angle of rotation of $\mathbf{B}$ [142], the local intermittency measure (LIM) [143] and the PVI [144]. LIM and PVI permit identification of large-amplitude bursts of magnetic energy at different time scales and at given times, namely in regions where the concentration of magnetic energy exceeds the average value over the entire dataset.

On the other hand, the solar wind turbulent cascade at the MHD scales has been observed to be intermittent, that is, the distributions of the magnetic field increments $\Delta\mathbf{B}(t,\tau) = \mathbf{B}(t+\tau) - \mathbf{B}(t)$ become more and more non-Gaussian as the time scale decreases [145,146]. This implies that

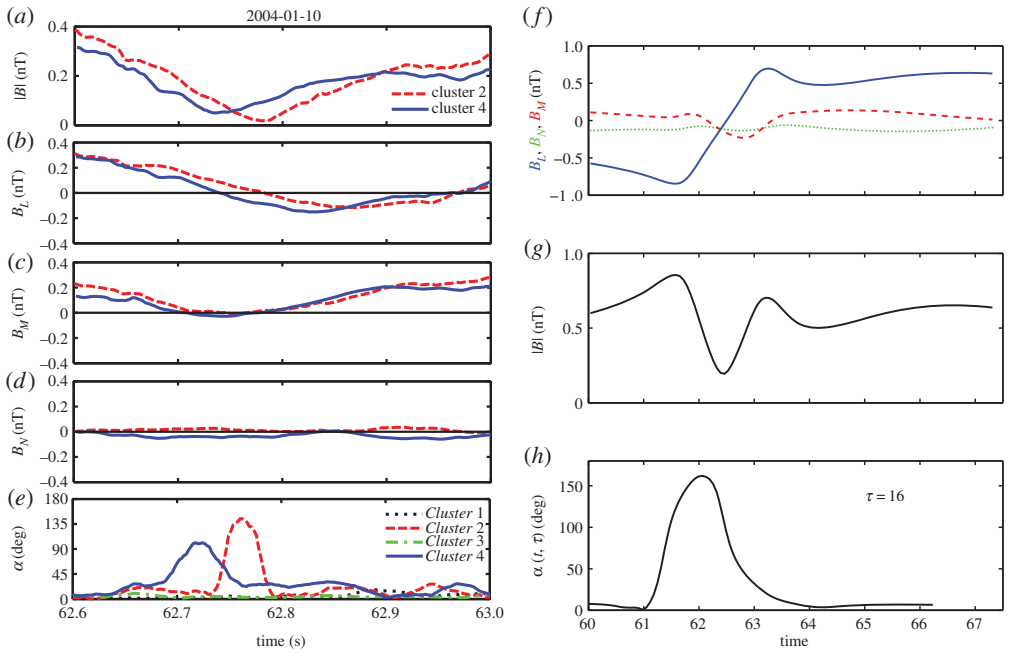

Figure 4. (*a*) Magnetic field magnitude as measured by STAFF on board *Cluster* 2 (red dashed line) and *Cluster* 4 (blue solid line), (*b*) the B_L component along the current sheet, (*c*) the B_M component out-of-plane, (*d*) the B_N component normal to the current sheet and (*e*) the angle of rotation $\alpha(t, \tau)$ as observed by all the four *Cluster* spacecraft. (*f*) Magnetic field components in the *LMN* reference frame from a two-dimensional Hall MHD simulation during a reconnecting current sheet, (*g*) the magnetic field intensity and (*h*) the angle of rotation. (Online version in colour.)

'extreme' values of the increments have a higher probability of occurrence as τ gets smaller. Those bursts in the magnetic field increments have been identified as regions of interface between portions of plasma having different speeds and bulk pressures, as MHD current sheets and as compressive discontinuities [138,147]. Thus, the turbulent cascade appears to generate localized structures that may extend to scales smaller than the proton inertial scale or gyroscale. The ion density data from *Spektr-R* also show pronounced intermittency [118,148], which increases, becoming very large in the inertial range, but stationary over the dissipation range. That behaviour matches that observed by the magnetic field [113,114].

The question now is how do magnetic structures observed at and below the proton scale influence intermittency at small scales? Recent studies on intermittency in that range of scales in the solar wind came to different conclusions: Alexandrova *et al.* [85] observed (using both FGM and STAFF data) a fourth-order moment of the distribution of the magnetic field increments that monotonically increased as the time scale decreased, indicating that the distributions became increasingly non-Gaussian. By contrast, Kiyani *et al.* [114], analysing a different solar wind interval of *Cluster* data, found that beyond the proton scale the distributions of the increments collapsed into a single shape, i.e. the statistics of the magnetic field increments becomes scale-invariant. A similar return to self-similarity has also been observed in both particle-in-cell (PIC) simulations and solar wind magnetic field data by Wu *et al.* [149]. Interestingly, a similar result was found by Chen *et al.* [148] using the data from *Spektr-R* [117]. Indeed, Chen *et al.* showed that the probability density functions of the plasma density increments are highly non-Gaussian at kinetic scales, but do not exhibit significant changes in the shape as a function of the time scale. Whether or not the origin of this time scale invariance in both the magnetic field and density in the kinetic range can be ascribed to sources of incoherent waves (cf. Wu *et al.* [149]) or to dissipation at current sheets (as suggested by Biskamp & Walter [150]) is not clear and needs further investigation.

6. Future missions that will address kinetic scale turbulence

As discussed above, high-resolution magnetic and plasma data obtained from *Cluster* and *Spektr-R* have allowed us to shed light on different new facets of kinetic turbulence, particularly as observed in the solar wind and Earth's magnetosheath. However, the same studies have exposed the limitations inherent in the available data and have highlighted the need for improving both the field and particle instrumentation. This is imperative if we are to advance our knowledge of kinetic processes in magnetofluid turbulence in general and space and astrophysical plasmas in particular. Those limitations arise because of the very small amplitudes of both the electric and magnetic field fluctuations in the solar wind at the dissipation scale and the difficulty of measuring velocity distribution functions of low-energy protons and electrons with high time resolution. One of these limitations is illustrated in figures 5 and 6. Figure 5 shows statistical results obtained from the magnetic energy spectra in the free streaming solar wind acquired by the *Cluster*/STAFF search coil magnetometer (SCM) at 30 Hz ($k\rho_e \sim 0.5$). To obtain an accurate spectrum, a signal-to-noise ratio exceeding 10 is desirable. The histogram shown in figure 5 is constructed from a survey of 10 years of burst mode data. It is clear that at 30 Hz the signal-to-noise ratio is commonly less than 10. Similarly, figure 6 compares the sensitivities of several search coil magnetometers, including the STAFF instrument, with a magnetic spectrum taken by *Cluster* in the solar wind. The relatively low sensitivities of the *MMS* and *THEMIS* search coils compared with that of *Cluster* is related to mass/power constraints on those two missions (the lengths of the coils were 27 cm, 18 cm and 10 cm on *Cluster*, *THEMIS* and *MMS*, respectively). This example shows that the *Cluster* SCM remains the most sensitive magnetometer ever flown and allows one to come close to capturing very low-amplitude magnetic fluctuations in the solar wind (note, however, that at ~100 Hz, because the signal reaches the noise floor, one cannot measure the electron gyrofrequency f_{ce} ~250 Hz).

The next major advance in space instrumentation will come with the launch of the *MMS* mission in the spring of 2015. That mission is designed to study the physics of magnetic reconnection at physical scales, approaching the electron inertial length, depending on the local plasma parameters. The particle instrumentation will be the most advanced yet flown and will have outstanding temporal resolution (150 ms for ions and 30 ms for electrons). Achieving similar resolution on other missions will be challenging, in no small part because of the current limitations on telemetry rates. Furthermore, to detect low-energy electrons, one must use techniques such as the Active Spacecraft Potential Control as on *Cluster* and *MMS*.

The four *MMS* spacecraft will be able to manoeuvre much closer together than was possible with *Cluster*. However, the primary mission of *MMS* is confined to the magnetosphere and magnetosheath. By the time that the orbit of the four spacecraft precesses into the solar wind, the prime mission will have ended and possible support for an extended mission will not be known for a couple of years. It is likely, as can be seen in figure 6, that the intrinsic noise of the search coil magnetometer will not be as low as that on *Cluster*.

In addition to *MMS*, the *DSCOVR* mission, launched by NASA in February 2015, will have instrumentation capable of monitoring the solar wind plasma at 0.5 s resolution and the magnetic field at 0.02 s resolution. The plasma instruments will provide higher time resolution data, including distribution functions, than has been generally available, but will not reach down to the dissipation range. The forthcoming NASA *Solar Probe Plus* mission (scheduled for launch in 2018) and the ESA–NASA *Solar Orbiter* mission [151] (scheduled for launch in 2017) will both have magnetic and electric field instrumentation capable of exploring in detail the dissipation range of the turbulence in the inner heliosphere (on *Solar Orbiter*) and the solar corona (*Solar Probe Plus*). The *Solar Probe Plus* search coil and electric field instruments are expected to be at least as good as those on *Cluster*; the electric and magnetic field instrumentation on *Solar Orbiter* is similar to that of *Solar Probe Plus*. However, the particle measurements of these two missions will have relatively low time resolution, especially in comparison with *MMS*. Thus, as indicated from figure 6, there does not appear to be any approved mission that will have both fields and particle instrumentation adequate to solve fully the dissipation problem—more sensitive

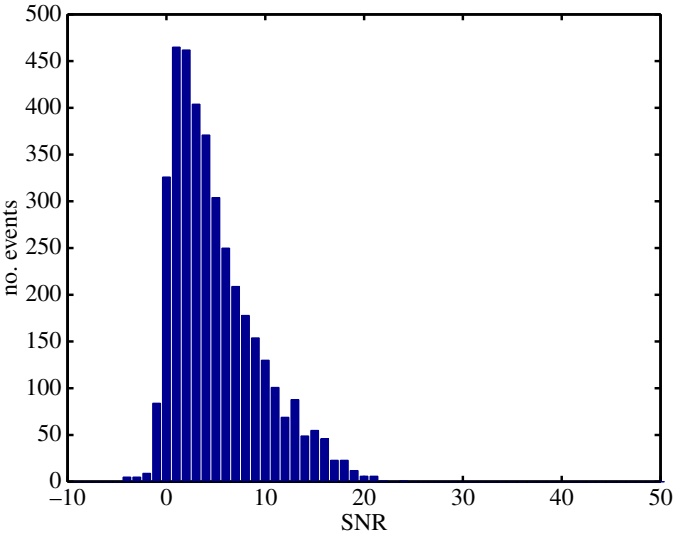

Figure 5. The distribution of the signal-to-noise ratio (SNR) of the magnetic energy in the spectrum of B_z (GSE) at $f = 30$ Hz. The data cover more than 10 years of *Cluster* STAFF burst mode data collected in the free streaming solar wind between 2001 and 2011. Note that SNR is defined as $\log(\delta B^2/B_s^2)$ where B_s is the sensitivity of the instrument at 30 Hz. Adapted from [128]. (Online version in colour.)

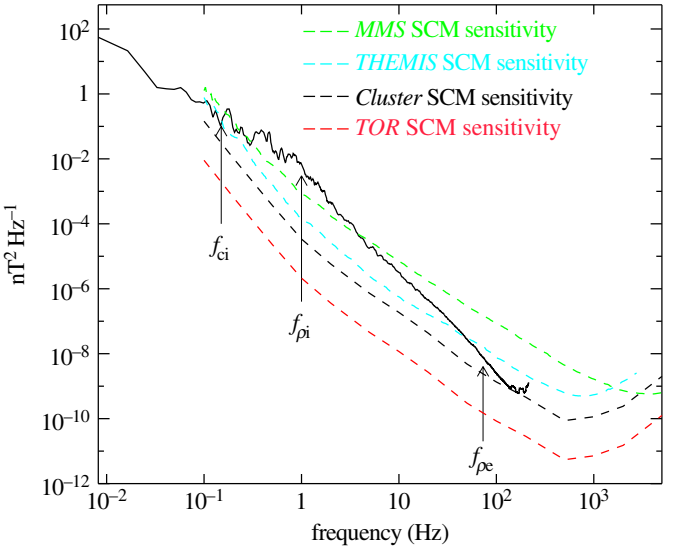

Figure 6. Comparison of sensitivities of search coil magnetometers on current and future missions. (The curve marked 'TOR' refers to an earlier proposal; the mission *THOR* now being studied will use that search coil magnetometer design.)

search coil magnetometers will be required for that task. A proposal designed to provide such an instrument is being prepared for a possible mission known as *THOR*. The proposal includes high cadence particle (especially electron) detectors. Measurements of three-dimensional (or even two-dimensional) electric field in the solar wind are indeed very challenging because of wake effects and the asymmetric photoelectron cloud. These two effects are reduced significantly for 'Sun-pointing' (i.e. the spin axis points towards the Sun) spacecraft, as proposed for *THOR*.

Acknowledgements. M.L.G. acknowledges the support of NASA headquarters to the *Cluster* mission.

Funding statement. R.T.W. is funded by a NASA GI grant and a NASA HSR grant at Goddard Space Flight Center. S.P.'s research is supported by 'Borsa Postdoc POR Calabria FSE 2007/2013'. F.S. was supported, in part, by the project THESOW funded by L'Agence Nationale de la Recherche (ANR, France).

References

1. Borrini G, Gosling JT, Bame SJ, Feldman WC, Wilcox JM. 1981 Solar wind helium and hydrogen structure near the heliospheric current sheet. *J. Geophys. Res.* **86**, 4565–4573. (doi:10.1029/JA086iA06p04565)
2. Parker EN. 1958 Dynamics of the interplanetary gas and magnetic fields. *Astrophys. J.* **128**, 664–676. (doi:10.1086/146579)
3. Gringauz KI. 1961 Some results of experiments in interplanetary space by means of charged particle traps on Soviet space probes. *Space Res.* **2**, 539–553.
4. Neugebauer M, Snyder CW. 1962 The mission of Mariner II: preliminary observations. *Science* **138**, 1095–1097. (doi:10.1126/science.138.3545.1095-a)
5. Unti TW, Neugebauer M. 1968 Alfvén waves in the solar wind. *Phys. Fluids* **11**, 563. (doi:10.1063/1.1691953)
6. Belcher JW, Davis LJ. 1971 Large-amplitude Alfvén waves in the interplanetary medium, 2. *J. Geophys. Res.* **76**, 3534–3563. (doi:10.1029/JA076i016p03534)
7. Coleman Jr PJ. 1966 Hydromagnetic waves in the interplanetary medium. *Phys. Rev. Lett.* **17**, 207. (doi:10.1103/PhysRevLett.17.207)
8. Coleman PJJ. 1968 Turbulence, viscosity, and dissipation in the solar-wind plasma. *Astrophys. J.* **153**, 371. (doi:10.1086/149674)
9. Matthaeus WH, Wan M, Servidio S, Greco A, Osman KT, Oughton S, Dmitruk P. 2015 Intermittency, nonlinear dynamics and dissipation in the solar wind and astrophysical plasmas. *Phil. Trans. R. Soc. A* **373**, 20140154. (doi:10.1098/rsta.2014.0154)
10. Kolmogorov AN. 1941 The local structure of turbulence in incompressible viscous fluid for very large Reynolds' numbers. *C. R. Dokl. Acad. Sci. URSS* **30**, 301–305.
11. Matthaeus WH, Goldstein ML. 1982 Measurement of the rugged invariants of magnetohydrodynamic turbulence in the solar wind. *J. Geophys. Res.* **87**, 6011–6028. (doi:10.1029/JA087iA08p06011)
12. Grant HL, Stewart RW, Moilliet A. 1962 Turbulence spectra from a tidal channel. *J. Fluid Mech.* **12**, 241–268. (doi:10.1017/S002211206200018X)
13. Roberts DA, Klein LW, Goldstein ML, Matthaeus WH. 1987 The nature and evolution of magnetohydrodynamic fluctuations in the solar wind: Voyager observations. *J. Geophys. Res.* **92**, 11 021–11 040. (doi:10.1029/JA092iA10p11021)
14. Roberts DA, Goldstein ML, Klein LW, Matthaeus WH. 1987 Origin and evolution of fluctuations in the solar wind: Helios observations and Helios–Voyager comparisons. *J. Geophys. Res.* **92**, 12 023–12 035. (doi:10.1029/JA092iA11p12023)
15. Leamon RJ, Matthaeus WH, Smith CW, Wong HK. 1998 Contribution of cyclotron-resonant damping to kinetic dissipation of interplanetary turbulence. *Astrophys. J.* **507**, L181–L184. (doi:10.1086/311698)
16. Marsch E, Vocks C, Tu CY. 2003 On ion-cyclotron-resonance heating of the corona and solar wind. *Nonlinear Processes Geophys.* **10**, 101–112. (doi:10.5194/npg-10-101-2003)
17. Hollweg JV 1983 Coronal heating by waves. In *JPL Solar Wind Five*, NASA Conf. Publ., vol. 228, pp. 5–22. Washington, DC: NASA.
18. Tu CY, Chen H. 1984 The heating of the solar wind by Alfvenic fluctuations. *Chin. J. Space Sci.* **4**, 277–284.
19. Gazis PR, Lazarus AJ. 1982 Voyager observations of solar wind proton temperature—1–10 AU. *Geophys. Res. Lett.* **9**, 431–434. (doi:10.1029/GL009i004p00431)
20. Gazis PR. 1984 Observations of plasma bulk parameters and the energy balance of the solar wind between 1 and 10 AU. *J. Geophys. Res.* **89**, 775–785. (doi:10.1029/JA089iA02p00775)
21. Verma MK, Roberts DA, Goldstein ML. 1995 Turbulent heating and temperature evolution of the solar wind plasma. *J. Geophys. Res.* **100**, 19839. (doi:10.1029/95JA01216)
22. Iroshnikov PS. 1962 Turbulence of a conducting fluid in a strong magnetic field. *Astron. Zh.* **40**, 742–750.
23. Kraichnan RH. 1965 Inertial-range spectrum of hydromagnetic turbulence. *Phys. Fluids* **8**, 1385–1387. (doi:10.1063/1.1761412)

24. Tu CY 1987 Explanation for the radial variation of the temperature of protons within the trailing edge of high speed streams between 1 and 5 AU. In *Proc. Sixth Int. Solar Wind Conf., Estes Park, CO, 23–28 August* (eds VJ Pizzo, T Holzer, DG Sime), NCAR Tech. Note NCAR/TN-306, vol. 2, p. 593. Boulder, CO: National Center for Atmospheric Research. (doi:10.5065/D6WS8R76)
25. Usmanov AV, Goldstein ML, Matthaeus WH. 2014 Three-fluid, three-dimensional magnetohydrodynamic solar wind model with eddy viscosity and turbulent resistivity. *Astrophys. J.* **788**, 43. (doi:10.1088/0004-637X/788/1/43)
26. Hollweg JV. 1974 On electron heat conduction in the solar wind. *J. Geophys. Res.* **79**, 3845–3850. (doi:10.1029/JA079i025p03845)
27. Hollweg JV. 1976 Collisionless electron heat conduction in the solar wind. *J. Geophys. Res.* **81**, 1649–1658. (doi:10.1029/JA081i010p01649)
28. MacBride BT, Smith CW. 2008 The turbulent cascade at 1 AU: energy transfer and the third-order scaling for MHD. *Astrophys. J.* **679**, 1644–1660. (doi:10.1086/529575)
29. Stawarz JE, Smith CW, Vasquez BJ, Forman MA, MacBride BT. 2009 The turbulent cascade and proton heating in the solar wind at 1 AU. *Astrophys. J.* **697**, 1119. (doi:10.1088/0004-637X/697/2/1119)
30. Coburn JT, Smith CW, Vasquez BJ, Stawarz JE, Forman MA. 2012 The turbulent cascade and proton heating in the solar wind during solar minimum. *Astrophys. J.* **754**, 93. (doi:10.1088/0004-637X/754/2/93)
31. Podesta JJ, Forman MA, Smith CW, Elton DC, Malécot Y, Gagne Y. 2009 Accurate estimation of third-order moments from turbulence measurements. *Nonlinear Processes Geophys.* **16**, 99–110. (doi:10.5194/npg-16-99-2009)
32. Leamon RJ, Smith CW, Ness NF, Wong HK. 1999 Dissipation range dynamics: kinetic Alfvén waves and the importance of β_e. *J. Geophys. Res.* **104**, 22 331–22 344. (doi:10.1029/1999JA900158)
33. Sahraoui F, Goldstein ML, Belmont G, Canu P, Rezeau L. 2010 Three dimensional anisotropic k spectra of turbulence at subproton scales in the solar wind. *Phys. Rev. Lett.* **105**, 131101. (doi:10.1103/PhysRevLett.105.131101)
34. Stawarz JE, Smith CW, Vasquez BJ, Forman MA, MacBride BT. 2010 The turbulent cascade for high cross-helicity states at 1 AU. *Astrophys. J.* **713**, 920. (doi:10.1088/0004-637X/713/2/920)
35. Smith CW, Stawarz JE, Vasquez BJ, Forman MA, MacBride BT. 2009 Turbulent cascade at 1 AU in high cross-helicity flows. *Phys. Rev. Lett.* **103**, 201101. (doi:10.1103/PhysRevLett.103.201101)
36. Matthaeus WH, Montgomery DC, Goldstein ML. 1983 Turbulent generation of outward-traveling interplanetary Alfvenic fluctuations. *Phys. Rev. Lett.* **51**, 1484–1487. (doi:10.1103/PhysRevLett.51.1484)
37. Podesta JJ. 2010 Comment on 'Turbulent cascade at 1 AU in high cross-helicity flows'. *Phys. Rev. Lett.* **104**, 169001. (doi:10.1103/PhysRevLett.104.169001)
38. Osman KT, Matthaeus WH, Greco A, Servidio S. 2011 Evidence for inhomogeneous heating in the solar wind. *Astrophys. J. Lett.* **727**, L11. (doi:10.1088/2041-8205/727/1/L11)
39. Borovsky JE, Denton MH. 2011 No evidence for heating of the solar wind at strong current sheets. *Astrophys. J. Lett.* **739**, L61. (doi:10.1088/2041-8205/739/2/L61)
40. Leamon RJ, Smith CW, Ness NF, Matthaeus WH, Wong HK. 1998 Observational constraints on the dynamics of the interplanetary magnetic field dissipation range. *J. Geophys. Res.* **103**, 4775–4787. (doi:10.1029/97JA03394)
41. Matthaeus WH, Goldstein ML, Smith C. 1982 Evaluation of magnetic helicity in homogeneous turbulence. *Phys. Rev. Lett.* **48**, 1256–1259. (doi:10.1103/PhysRevLett.48.1256)
42. Bruno R, Trenchi L. 2014 Radial dependence of the frequency break between fluid and kinetic scales in the solar wind fluctuations. *Astrophys. J. Lett.* **787**, L24. (doi:10.1088/2041-8205/787/2/L24)
43. Goldstein ML, Roberts DA, Fitch CA. 1994 Properties of the fluctuating magnetic helicity in the inertial and dissipation ranges of solar wind turbulence. *J. Geophys. Res.* **99**, 11 519–11 538. (doi:10.1029/94JA00789)
44. Moffatt HK. 1978 *Magnetic field generation in electrically conducting fluids*. Cambridge, UK: Cambridge University Press.
45. TenBarge JM, Howes GG, Dorland W. 2013 Collisionless damping at electron scales in solar wind turbulence. *Astrophys. J.* **774**, 139. (doi:10.1088/0004-637X/774/2/139)

46. Dum CT, Marsch E, Pilipp W. 1980 Determination of wave growth from measured distribution functions and transport theory. *J. Plasma Phys.* **23**, 91–113. (doi:10.1017/S0022377800022170)
47. Podesta JJ. 2012 The need to consider ion Bernstein waves as a dissipation channel of solar wind turbulence. *J. Geophys. Res.* **117**, A07101. (doi:10.1029/2012JA017770)
48. Cranmer SR, van Ballegooijen AA. 2003 Alfvénic turbulence in the extended solar corona: kinetic effects and proton heating. *Astrophys. J.* **594**, 573–591. (doi:10.1086/376777)
49. Mithaiwala M, Rudakov L, Crabtree C, Ganguli G. 2012 Co-existence of whistler waves with kinetic Alfven wave turbulence for the high-beta solar wind plasma. *Phys. Plasmas* **19**, 102902. (doi:10.1063/1.4757638)
50. He J, Marsch E, Tu C, Yao S, Tian H. 2011 Possible evidence of Alfvén-cyclotron waves in the angle distribution of magnetic helicity of solar wind turbulence. *Astrophys. J.* **731**, 85. (doi:10.1088/0004-637X/731/2/85)
51. He J, Tu C, Marsch E, Yao S. 2011 Do oblique Alfvén/ion-cyclotron or fast-mode/whistler waves dominate the dissipation of solar wind turbulence near the proton inertial length? *Astrophys. J.* **745**, L8. (doi:10.1088/2041-8205/745/1/L8)
52. Jian LK *et al.* 2014 Electromagnetic waves near the proton cyclotron frequency: STEREO observations. *Astrophys. J.* **786**, 123. (doi:10.1088/0004-637X/786/2/123)
53. Podesta JJ, Gary SP. 2011 Effect of differential flow of alpha particles on proton pressure anisotropy instabilities in the solar wind. *Astrophys. J.* **742**, 41. (doi:10.1088/0004-637X/742/1/41)
54. Klein KG, Howes GG, TenBarge JM, Podesta JJ. 2014 Physical interpretation of the angle-dependent magnetic helicity spectrum in the solar wind: the nature of turbulent fluctuations near the proton gyroradius scale. *Astrophys. J.* **785**, 138. (doi:10.1088/0004-637X/785/2/138)
55. Leamon RJ, Matthaeus WH, Smith CW, Zank GP, Mullan DJ, Oughton S. 2000 MHD-driven kinetic dissipation in the solar wind and corona. *Astrophys. J.* **537**, 1054–1062. (doi:10.1086/309059)
56. Kaghashvili EK. 1999 Ion-cyclotron wave dissipation channel for Alfvén waves. *Geophys. Res. Lett.* **26**, 1817–1820. (doi:10.1029/1999GL900343)
57. Marsch E, Tu CY. 1997 The effects of high-frequency Alfven waves on coronal heating and solar wind acceleration. *Astron. Astrophys.* **319**, L17–L20. See http://adsabs.harvard.edu/full/1997A%26A...319L..17M.
58. Osman KT, Matthaeus WH, Kiyani KH, Hnat B, Chapman SC. 2013 Proton kinetic effects and turbulent energy cascade rate in the solar wind. *Phys. Rev. Lett.* **111**, 201101. (doi:10.1103/PhysRevLett.111.201101)
59. Cranmer SR, Asgari-Targhi M, Miralles MP, Raymond JC, Strachan L, Tian H, Woolsey LN. 2015 The role of turbulence in coronal heating and solar wind expansion. *Phil. Trans. R. Soc. A* **373**, 20140148. (doi:10.1098/rsta.2014.0148)
60. Isenberg PA. 1984 Resonant acceleration and heating of solar wind ions: anisotropy and dispersion. *J. Geophys. Res.* **89**, 6613–6622. (doi:10.1029/JA089iA08p06613)
61. Isenberg PA. 1990 Investigations of a turbulence-driven solar wind model. *J. Geophys. Res.* **95**, 6437–6442. (doi:10.1029/JA095iA05p06437)
62. Isenberg PA, Lee MA, Hollweg JV. 2000 A kinetic model of coronal heating and acceleration by ion-cyclotron waves: preliminary results. *Solar Phys.* **193**, 247–257. (doi:10.1023/A:1005253706166)
63. Isenberg PA. 2001 Heating of coronal holes and generation of the solar wind by ion-cyclotron resonance. *Space Sci. Rev.* **95**, 119–131. (doi:10.1023/A:1005287225222)
64. Isenberg PA, Lee MA, Hollweg JV. 2001 The kinetic shell model of coronal heating and acceleration by ion cyclotron waves: 1. Outward propagating waves. *J. Geophys. Res.* **106**, 5649–5660. (doi:10.1029/2000JA000099)
65. Isenberg PA. 2001 The kinetic shell model of coronal heating and acceleration by ion cyclotron waves: 2. Inward and outward propagating waves. *J. Geophys. Res.* **106**, 29 249–29 260. (doi:10.1029/2001JA000176)
66. Hollweg JV, Isenberg PA. 2002 Generation of the fast solar wind: a review with emphasis on the resonant cyclotron interaction. *J. Geophys. Res.* **107**, 1147. (doi:10.1029/2001JA000270)
67. Isenberg PA. 2004 The kinetic shell model of coronal heating and acceleration by ion cyclotron waves: 3. The proton halo and dispersive waves. *J. Geophys. Res.* **109**, 3101. (doi:10.1029/2002JA009449)

68. Isenberg PA. 2004 Correction to 'The kinetic shell model of coronal heating and acceleration by ion cyclotron waves: 3. The proton halo and dispersive waves'. *J. Geophys. Res.* **109**, 6106. (doi:10.1029/2004JA010524)
69. Isenberg PA, Vasquez BJ. 2011 A kinetic model of solar wind generation by oblique ion-cyclotron waves. *Astrophys. J.* **731**, 88. (doi:10.1088/0004-637X/731/2/88)
70. Tu CY, Marsch E. 1997 Two-fluid model for heating of the solar corona and acceleration of the solar wind by high-frequency Alfven waves. *Solar Phys.* **171**, 363–391. (doi:10.1023/A:1004968327196)
71. Marsch E. 1998 Cyclotron heating of the solar corona. *Astrophys. Space Sci.* **264**, 63–76. (doi:10.1023/A:1002436407996)
72. Marsch E, Tu CY. 2001 Heating and acceleration of coronal ions interacting with plasma waves through cyclotron and Landau resonance. *J. Geophys. Res.* **106**, 227–238. (doi:10.1029/2000JA000042)
73. Tu CY, Marsch E. 2001 On cyclotron wave heating and acceleration of solar wind ions in the outer corona. *J. Geophys. Res.* **106**, 8233–8252. (doi:10.1029/2000JA000024)
74. Bourouaine S, Marsch E, Vocks C. 2008 On the efficiency of nonresonant ion heating by coronal Alfvén waves. *Astrophys. J. Lett.* **684**, L119–L122. (doi:10.1086/592243)
75. Sahraoui F, Goldstein ML, Robert P, Khotyaintsev YV. 2009 Evidence of a cascade and dissipation of solar-wind turbulence at the electron gyroscale. *Phys. Rev. Lett.* **102**, 231102. (doi:10.1103/PhysRevLett.102.231102)
76. Howes GG, Cowley SC, Dorland W, Hammett GW, Quataert E, Schekochihin AA. 2008 A model of turbulence in magnetized plasmas: implications for the dissipation range in the solar wind. *J. Geophys. Res.* **113**, A05103. (doi:10.1029/2007JA012665)
77. Schekochihin AA, Cowley SC, Dorland W, Hammett GW, Howes GG, Quataert E, Tatsuno T. 2009 Astrophysical gyrokinetics: kinetic and fluid turbulent cascades in magnetized weakly collisional plasmas. *Astrophys. J. Suppl.* **182**, 310–377. (doi:10.1088/0067-0049/182/1/310)
78. Gary SP, Borovsky JE. 2004 Alfvén-cyclotron fluctuations: linear Vlasov theory. *J. Geophys. Res.* **109**, 6105. (doi:10.1029/2004JA010399)
79. Biskamp D, Schwarz E, Drake JF. 1996 Two-dimensional electron magnetohydrodynamic turbulence. *Phys. Rev. Lett.* **76**, 1264–1267. (doi:10.1103/PhysRevLett.76.1264)
80. Servidio S, Carbone V, Primavera L, Veltri P, Stasiewicz K. 2007 Compressible turbulence in Hall magnetohydrodynamics. *Planet. Space Sci.* **55**, 2239–2243. (doi:10.1016/j.pss.2007.05.023)
81. Dmitruk P, Matthaeus WH, Seenu N. 2004 Test particle energization by current sheets and nonuniform fields in magnetohydrodynamic turbulence. *Astrophys. J.* **617**, 667–679. (doi:10.1086/425301)
82. Markovskii SA, Vasquez BJ, Smith CW. 2008 Statistical analysis of the high-frequency spectral break of the solar wind turbulence at 1 AU. *Astrophys. J.* **675**, 1576–1583. (doi:10.1086/527431)
83. Perri S, Carbone V, Veltri P. 2010 Where does fluid-like turbulence break down in the solar wind? *Astrophys. J. Lett.* **725**, L52–L55. (doi:10.1088/2041-8205/725/1/L52)
84. Galtier S. 2006 Wave turbulence in incompressible Hall magnetohydrodynamics. *J. Plasma Phys.* **72**, 721–769. (doi:10.1017/S0022377806004521)
85. Alexandrova O, Carbone V, Veltri P, Sorriso-Valvo L. 2008 Small-scale energy cascade of the solar wind turbulence. *Astrophys. J.* **674**, 1153–1157. (doi:10.1086/524056)
86. Bourouaine S, Alexandrova O, Marsch E, Maksimovic M. 2012 On spectral breaks in the power spectra of magnetic fluctuations in the fast solar wind between 0.3 and 0.9 AU. *Astrophys. J.* **749**, 102. (doi:10.1088/0004-637X/749/2/102)
87. Chen CHK, Leung L, Boldyrev S, Maruca BA, Bale SD. 2014 Ion scale spectral break of solar wind turbulence at high and low beta. *Geophys. Res. Lett.* **41**, 8081–8088. (doi:10.1002/2014GL062009)
88. Galtier S, Meyrand R. 2014 Entanglement of helicity and energy in kinetic Alfvén wave/whistler turbulence. *J. Plasma Phys.* **81**, 1–27. (doi:10.1017/S0022377814000774)
89. Taylor GI 1938 The spectrum of turbulence. *Proc. R. Soc. Lond. A* **164**, 476–490. (doi:10.1098/rspa.1938.0032)
90. Horbury TS, Forman M, Oughton S. 2008 Anisotropic scaling of magnetohydrodynamic turbulence. *Phys. Rev. Lett.* **101**, 175005. (doi:10.1103/PhysRevLett.101.175005)
91. Podesta JJ. 2009 Dependence of solar-wind power spectra on the direction of the local mean magnetic field. *Astrophys. J.* **698**, 986. (doi:10.1088/0004-637X/698/2/986)

92. Luo QY, Wu DJ. 2010 Observations of anisotropic scaling of solar wind turbulence. *Astrophys. J. Lett.* **714**, L138–L141. (doi:10.1088/2041-8205/714/1/L138)
93. Wicks RT, Horbury TS, Chen CHK, Schekochihin AA. 2010 Power and spectral index anisotropy of the entire inertial range of turbulence in the fast solar wind. *Mon. Not. R. Astron. Soc.* **407**, L31–L35. (doi:10.1111/j.1745-3933.2010.00898.x)
94. Forman MA, Wicks RT, Horbury TS. 2011 Detailed fit of 'critical balance' theory to solar wind turbulence measurements. *Astrophys. J.* **733**, 76. (doi:10.1088/0004-637X/733/2/76)
95. Koval A, Szabo A 2013 Magnetic field turbulence spectra observed by the Wind spacecraft. In *Solar Wind 13: Proc. Thirteenth Int. Solar Wind Conf., Big Island, Hawaii, 17–22 June* (eds GP Zank *et al.*), AIP Conf. Proc., vol. 1539, pp. 211–214. New York, NY: American Institute of Physics. (doi:10.1063/1.4811025)
96. Escoubet CP, Fehringer M, Goldstein ML. 2001 The Cluster mission. *Ann. Geophys.* **19**, 1197–1200. (doi:10.5194/angeo-19-1197-2001)
97. Pinçon JL, Lefeuvre F. 1988 Characterization of a homogeneous field turbulence from multipoint measurements. *Adv. Space Res.* **8**, 459–462. (doi:10.1016/0273-1177(88)90161-5)
98. Pinçon JL, Lefeuvre F. 1991 Local characterization of homogeneous turbulence in a space plasma from simultaneous measurements of field components at several points in space. *J. Geophys. Res.* **96**, 1789–1802. (doi:10.1029/90JA02183)
99. Pinçon JL, Lefeuvre F. 1992 The application of the generalized Capon method to the analysis of a turbulent field in space plasma: experimental constraints. *J. Atmos. Terr. Phys.* **54**, 1237–1247. (doi:10.1016/0021-9169(92)90032-G)
100. Pinçon JL, Motschmann U. 1998 Multi-spacecraft filtering: general framework. In *Analysis methods for multi-spacecraft data* (eds G Paschmann, PW Daly), pp. 79–91. Noordwijk, The Netherlands: ESA Publications Division.
101. Neubauer F, Glassmeier KH. 1987 Use of an array of satellites as a wave telescope. *J. Geophys. Res.* **95**, 19 115–19 122. (doi:10.1029/JA095iA11p19115)
102. Matthaeus WH, Goldstein ML. 1982 Stationarity of magnetohydrodynamic fluctuations in the solar wind. *J. Geophys. Res.* **87**, 10 347–10 354. (doi:10.1029/JA087iA12p10347)
103. Perri S, Goldstein M, Dorelli J, Sahraoui F. 2012 Detection of small-scale structures in the dissipation regime of solar-wind turbulence. *Phys. Rev. Lett.* **109**, 191101. (doi:10.1103/PhysRevLett.109.191101)
104. Retinò A, Sundkvist D, Vaivads A, Mozer F, André M, Owen CJ. 2007 *In situ* evidence of magnetic reconnection in turbulent plasma. *Nat. Phys.* **3**, 235–238. (doi:10.1038/nphys574)
105. Sundkvist D, Retinò A, Vaivads A, Bale SD. 2007 Dissipation in turbulent plasma due to reconnection in thin current sheets. *Phys. Rev. Lett.* **99**, 025004. (doi:10.1103/PhysRevLett.99.025004)
106. Huang SY, Zhou M, Deng XH, Yuan ZG, Pang Y, Wei Q, Su W, Li HM, Wang QQ. 2012 Kinetic structure and wave properties associated with sharp dipolarization front observed by Cluster. *Ann. Geophys.* **30**, 97–107. (doi:10.5194/angeo-30-97-2012)
107. Huang SY *et al.* 2012 Observations of turbulence within reconnection jet in the presence of guide field. *Geophys. Res. Lett.* **39**, L11104. (doi:10.1029/2012GL052210)
108. Narita Y, Glassmeier KH, Sahraoui F, Goldstein ML. 2010 Wave-vector dependence of magnetic-turbulence spectra in the solar wind. *Phys. Rev. Lett.* **104**, 171101. (doi:10.1103/PhysRevLett.104.171101)
109. Chen CHK, Mallet A, Schekochihin AA, Horbury TS, Wicks RT, Bale SD. 2012 Three-dimensional structure of solar wind turbulence. *Astrophys. J.* **758**, 120. (doi:10.1088/0004-637X/758/2/120)
110. Chen CHK, Horbury TS, Schekochihin AA, Wicks RT, Alexandrova O, Mitchell J. 2010 Anisotropy of solar wind turbulence between ion and electron scales. *Phys. Rev. Lett.* **104**, 255002. (doi:10.1103/PhysRevLett.104.255002)
111. Lacombe C, Alexandrova O, Matteini L, Santolik O, Cornilleau-Wehrlin N, Mangeney A, de Conchy Y, Maksimovic M. 2014 Whistler mode waves and the electron heat flux in the solar wind: Cluster observations. *Astrophys. J.* **796**, 5. (doi:10.1088/0004-637X/796/1/5)
112. Alexandrova O, Lacombe C, Mangeney A, Grappin R, Maksimovic M. 2012 Solar wind turbulent spectrum at plasma kinetic scales. *Astrophys. J.* **760**, 121. (doi:10.1088/0004-637X/760/2/121)

113. Kiyani KH, Chapman SC, Sahraoui F, Hnat B, Fauvarque O, Khotyaintsev YV. 2013 Enhanced magnetic compressibility and isotropic scale invariance at sub-ion Larmor scales in solar wind turbulence. *Astrophys. J.* **763**, 10. (doi:10.1088/0004-637X/763/1/10)
114. Kiyani K, Chapman S, Khotyaintsev Y, Dunlop M, Sahraoui F. 2009 Global scale-invariant dissipation in collisionless plasma turbulence. *Phys. Rev. Lett.* **103**, 075006. (doi:10.1103/PhysRevLett.103.075006)
115. Alexandrova O, Saur J, Lacombe C, Mangeney A, Mitchell J, Schwartz SJ, Robert P. 2009 Universality of solar-wind turbulent spectrum from MHD to electron scales. *Phys. Rev. Lett.* **103**, 165003. (doi:10.1103/PhysRevLett.103.165003)
116. Kiyani K, Chapman S, Khotyaintsev Y, Dunlop M, Sahraoui F. 2010 Fractal dissipation of small-scale magnetic fluctuations in solar wind turbulence as seen by Cluster. In *Proc. Twelfth Int. Solar Wind Conf., Saint-Malo, France, 21–26 June* (eds M Maksomovic *et al.*), AIP Conf. Proc., vol. 1216, pp. 136–139. New York, NY: American Institute of Physics. (doi:10.1063/1.3395819)
117. Šafránková J, Němeček Z, Přech L, Zastenker GN. 2013 Ion kinetic scale in the solar wind observed. *Phys. Rev. Lett.* **110**, 025004. (doi:10.1103/PhysRevLett.110.025004)
118. Riazantseva MO, Budaev VP, Zelenyi LM, Zastenker GN, Pavlos GP, Safrankova J, Nemecek Z, Prech L, Nemec F. 2015 Dynamic properties of small-scale solar wind plasma fluctuations. *Phil. Trans. R. Soc. A* **373**, 20140146. (doi:10.1098/rsta.2014.0146)
119. Chen CHK, Salem CS, Bonnell JW, Mozer FS, Bale SD. 2012 Density fluctuation spectrum of solar wind turbulence between ion and electron scales. *Phys. Rev. Lett.* **109**, 035001. (doi:10.1103/PhysRevLett.109.035001)
120. Camporeale E, Burgess D. 2011 The dissipation of solar wind turbulent fluctuations at electron scales. *Astrophys. J.* **730**, 114. (doi:10.1088/0004-637X/730/2/114)
121. Camporeale E, Burgess D. 2011 Erratum: 'The dissipation of solar wind turbulent fluctuations at electron scales' (2011, ApJ, 730, 114). *Astrophys. J.* **735**, 67. (doi:10.1088/0004-637X/735/1/67)
122. Howes GG, TenBarge JM, Dorland W, Quataert E, Schekochihin AA, Numata R, Tatsuno T. 2011 Gyrokinetic simulations of solar wind turbulence from ion to electron scales. *Phys. Rev. Lett.* **107**, 35004. (doi:10.1103/PhysRevLett.107.035004)
123. Chang O, Gary SP, Wang J. 2011 Whistler turbulence forward cascade: three-dimensional particle-in-cell simulations. *Geophys. Res. Lett.* **38**, 22102. (doi:10.1029/2011GL049827)
124. Meyrand R, Galtier S. 2010 A universal law for solar-wind turbulence at electron scales. *Astrophys. J.* **721**, 1421–1424. (doi:10.1088/0004-637X/721/2/1421)
125. Podesta JJ, Borovsky JE, Gary SP. 2010 A kinetic Alfvén wave cascade subject to collisionless damping cannot reach electron scales in the solar wind at 1 AU. *Astrophys. J.* **712**, 685–691. (doi:10.1088/0004-637X/712/1/685)
126. Sahraoui F, Belmont G, Goldstein ML. 2012 New insight into short-wavelength solar wind fluctuations from Vlasov theory. *Astrophys. J.* **748**, 100. (doi:10.1088/0004-637X/748/2/100)
127. Meyrand R, Galtier S. 2012 Spontaneous chiral symmetry breaking of Hall magneto-hydrodynamic turbulence. *Phys. Rev. Lett.* **109**, 194501. (doi:10.1103/PhysRevLett.109.194501)
128. Sahraoui F, Huang SY, Belmont G, Goldstein ML, Retinó A, Robert P, Cornilleau-Wehrlin N, DePatoul J. 2013 Scaling of the electron dissipation range of solar wind turbulence. *Astrophys. J.* **777**, 15. (doi:10.1088/0004-637X/777/1/15)
129. Bale SD, Kellogg PJ, Mozer FS, Horbury TS, Rème H. 2005 Measurement of the electric fluctuation spectrum of magnetohydrodynamic turbulence. *Phys. Rev. Lett.* **94**, 215002. (doi:10.1103/PhysRevLett.94.215002)
130. Chen CHK, Boldyrev S, Xia Q, Perez JC. 2013 Nature of subproton scale turbulence in the solar wind. *Phys. Rev. Lett.* **110**, 225002. (doi:10.1103/PhysRevLett.110.225002)
131. Salem CS, Howes GG, Sundkvist D, Bale SD, Chaston CC, Chen CHK, Mozer FS. 2012 Identification of kinetic Alfvén wave turbulence in the solar wind. *Astrophys. J. Lett.* **745**, L9. (doi:10.1088/2041-8205/745/1/L9)
132. Podesta JJ. 2013 Evidence of kinetic Alfvén waves in the solar wind at 1 AU. *Solar Phys.* **286**, 529–548. (doi:10.1007/s11207-013-0258-z)
133. Howes GG, Klein KG, TenBarge JM. 2014 Validity of the Taylor hypothesis for linear kinetic waves in the weakly collisional solar wind. *Astrophys. J.* **789**, 106. (doi:10.1088/0004-637X/789/2/106)

134. Burlaga LF, Ness NF. 1969 Tangential discontinuities in the solar wind. *Solar Phys.* **9**, 467–477. (doi:10.1007/BF02391672)
135. Tsurutani BT, Smith EJ. 1979 Interplanetary discontinuities—temporal variations and the radial gradient from 1 to 8.5 AU. *J. Geophys. Res.* **84**, 2773–2787. (doi:10.1029/JA084iA06p02773)
136. Li G. 2008 Identifying current-sheet-like structures in the solar wind. *Astrophys. J. Lett.* **672**, L65–L68. (doi:10.1086/525847)
137. Mariani F, Bavassano B, Villante U, Ness NF. 1973 Variations of the occurrence rate of discontinuities in the interplanetary magnetic field. *J. Geophys. Res.* **78**, 8011. (doi:10.1029/JA078i034p08011)
138. Bruno R, Carbone V, Veltri P, Pietropaolo E, Bavassano B. 2001 Identifying intermittency events in the solar wind. *Planet. Space Sci.* **49**, 1201–1210. (doi:10.1016/S0032-0633(01)00061-7)
139. Borovsky JE. 2008 Flux tube texture of the solar wind: strands of the magnetic carpet at 1 AU? *J. Geophys. Res.* **113**, 8110. (doi:10.1029/2007JA012684)
140. Greco A, Matthaeus WH, Servidio S, Chuychai P, Dmitruk P. 2009 Statistical analysis of discontinuities in solar wind ACE data and comparison with intermittent MHD turbulence. *Astrophys. J. Lett.* **691**, L111–L114. (doi:10.1088/0004-637X/691/2/L111)
141. Greco A, Perri S. 2014 Identification of high shears and compressive discontinuities in the inner heliosphere. *Astrophys. J.* **784**, 163. (doi:10.1088/0004-637X/784/2/163)
142. Zhdankin V, Boldyrev S, Mason J. 2012 Distribution of magnetic discontinuities in the solar wind and in magnetohydrodynamic turbulence. *Astrophys. J. Lett.* **760**, L22. (doi:10.1088/2041-8205/760/2/L22)
143. Farge M, Guezennec Y, Ho CM, Meneveau C. 1990 Continuous wavelet analysis of coherent structures. In *Studying turbulence using numerical simulation databases. 3: proceedings of the 1990 summer program* (ed. D Spinks), pp. 331–348. Stanford, CA: Stanford University.
144. Greco A, Chuychai P, Matthaeus WH, Servidio S, Dmitruk P. 2008 Intermittent MHD structures and classical discontinuities. *Geophys. Res. Lett.* **35**, 19111. (doi:10.1029/2008GL035454)
145. Marsch E, Tu CY. 1997 Intermittency, non-Gaussian statistics and fractal scaling of MHD fluctuations in the solar wind. *Nonlinear Processes Geophys.* **4**, 101–124. (doi:10.5194/npg-4-101-1997)
146. Sorriso-Valvo L, Carbone V, Veltri P, Consolini G, Bruno R. 1999 Intermittency in the solar wind turbulence through probability distribution functions of fluctuations. *Geophys. Res. Lett.* **26**, 1801–1804. (doi:10.1029/1999GL900270)
147. Veltri P, Nigro G, Malara F, Carbone V, Mangeney A. 2005 Intermittency in MHD turbulence and coronal nanoflares modelling. *Nonlinear Processes Geophys.* **12**, 245–255. (doi:10.5194/npg-12-245-2005)
148. Chen CHK, Sorriso-Valvo L, Šafránková J, Němeček Z. 2014 Intermittency of solar wind density fluctuations from ion to electron scales. *Astrophys. J. Lett.* **789**, L8. (doi:10.1088/2041-8205/789/1/L8)
149. Wu P, Perri S, Osman K, Wan M, Matthaeus WH, Shay MA, Goldstein ML, Karimabadi H, Chapman S. 2013 Intermittent heating in solar wind and kinetic simulations. *Astrophys. J. Lett.* **763**, L30. (doi:10.1088/2041-8205/763/2/L30)
150. Biskamp D, Welter H, Walter M. 1990 Statistical properties of two-dimensional magnetohydrodynamic turbulence. *Phys. Fluids B* **2**, 3024–3031. (doi:10.1063/1.859369)
151. Müller D, Marsden RG, St Cyr OC, Gilbert HR. 2013 Solar Orbiter exploring the Sun–heliosphere connection. *Solar Phys.* **285**, 25–70. (doi:10.1007/s11207-012-0085-7)